ASSESSMENT OF PID-BASED CONTROL OF SERVO-ACTUATORS FOR FLIGHT REGULATION OF SMALL UNMANNED AERIAL VEHICLES

Mahmud S. Zango [1], Ameer Mohammed[2]*, Jamilu U. Yahaya [2], Khalid K Dandago[1], [2]Muhammad I Muhammad [2],Abdulbasit Hassan[1]
[1]Aerospace Engineering Department, Air Force Institute of Technology, Kaduna – Nigeria.
[2]Mechatronic Engineering Department, Air Force Institute of Technology, Kaduna– Nigeria.
*m.ameer@afit.edu.ng

Keywords: –
Controller, Proportional-Velocity, Proportional-Integral, Servomotor, Unmanned Aerial Vehicles.

Article History: –
Received: March, 2021.
Reviewed: June, 2021
Accepted: August, 2021
Published: September, 2021.

ABSTRACT

Flight control systems for unmanned aerial vehicles (UAVs) are responsible for maintaining safe flight – they are required to be reliable and robust. Flight regulation is achieved by controlling servomotors linked to flight control surfaces – ailerons, rudder, elevators and flaps. The most important parameters in servomotor control are position and speed. Hence, this work performed an assessment of proportional integral and derivative based controllers for servo motors used in attitude control of UAVs. In the experiment, the performance of proportional-velocity (PV) position and proportional-integral (PI) speed controllers were investigated by studying the impact of the individual gains on the dynamics of the systems. Both PV position and PI speed controllers demonstrated satisfactory performance with few challenges including presence of measurement noise and steady state error. The PV position controller addressed these challenges with its superior noise suppression ability. This makes it more ideal for controlling servo actuators of flight control surfaces.

1. INTRODUCTION

Unmanned Aerial Vehicles (UAVs) are increasingly adopted for use in diverse applications including precision agriculture [1], [2] search and rescue missions, security and surveillance [3], [4], remote sensing [5] and many more. The flight control system (FCS), a vital systems in UAVs is responsible for controlling its direction and attitude. In the case of fixed-wing UAVs, control is achieved using some actuators linked to the control surfaces. In rotary-wing UAVs, attitude control is achieved by regulating the speed and direction of rotation of individual motors. Considering the importance of actuators in UAV control, ensuring their efficient operation is necessary. Some of the most significant problems that affect servo control include noise disturbances from signal measurement, higher order controller equations, and decoupling problems [6]. Various control approaches have been proposed to addressed these problems. One of the most common control structure used for FCS is the classic proportional, integral, and derivative PID control. PID control have been used for many decades in industries and formed more than 90% of industrial control loops due to their simplicity, robustness and performance [7], [8]. PID control has been adopted in many commercial flight control systems for UAV attitude control [9], [10]. PID controller or variants have been used in [6], [8], [11], [12] for attitude control of rotary-wing UAV with great performance. However, one common challenge to these approaches is the dynamic nature of disturbance to the system introduced from measurement signals.

Another approach is to design FCS based on Non-linear Inverse Dynamics. This method offers improved performance and safety in comparison with linearization, by addressing the non-linearity in the UAV model. However, it can only be used when the exact plant and external disturbances models are known. But in reality, these models are dynamic in nature and are only approximations of the real systems they represent. Therefore in such cases adaptive control algorithms are the preferred solutions as used in [13], [14][15].

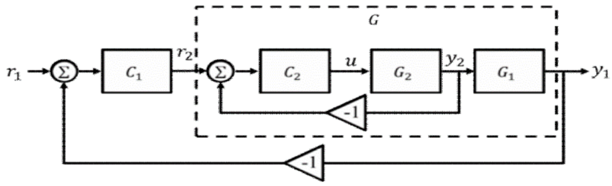

Fig. 1: General Cascade Control Structure.

Cascade PID control has been proposed to addressed attitude control problems of the FCS [6], [8], [11], [12]. This control structure is an advance form of PID control which find many applications in motor control, process control and automation. Cascade control structure contains two control loops as shown in Fig. 1: the inner (secondary) and outer (primary) control loops. The control approach is ideal when the dynamics of the secondary loop are faster than that of the primary loop. Cascade control is easy to understand and implement, resilient to load disturbance from measurement signals, and improve response time.

Consequently, this work will evaluate different PID algorithms for optimal control of speed and position of servo motor using cascade control structure. Cascade control structure is proposed due to its capability of rejecting external disturbances and improvement of performance [6]. The focus of the work will be on ensuring faster dynamics, handling of non-linearities and noise disturbance suppression in the secondary control loop of the cascade control structure, which is common in the control of flight control surface. The rest of the paper is organized as follows: Section II presents more detail on the servo testbench and PID variants. The result obtained from the experiment are presented in Section III, while Section IV provide further discussion. Concluding remarks are provided in Section IV.

1. SERVO TESTBENCH AND PID VARIANTS

Servo-systems are high accuracy devices that utilize negative feedback system to control mechanical position, speed or acceleration[16]. Some characteristics of servo system are high torque (at stand still), long range of speed control, great accuracy, low torque ripple and speed control [16], [5], [17].

The inherent non-linearities associated with servo motors coupled with external noise disturbances complicate their speed and position control. A number of solutions have been proposed in the literature including fractional order controllers and its variants [18], [19]; and fuzzy logic controllers [20]–[23]. These controllers all presented improved performance but often require sophisticated tuning algorithms [24][25][26]. This makes it less attractive to adopt these algorithms. Hence, it is necessary to devise new solutions that are simple and easy to implement like the PID and its variants, which are explored in this work.

2.1 Servo testbench

A Quanser QUBE-Servo Mechanism is the servo system used in this experiment. The schematic of its armature is presented in Fig. 2 and its parameters are given in Table 1. The shaft of the motor is linked to load in form of a metal disk which is used to mount the rotary pendulum. The moment of inertia of the load is denoted by J_d. The back emf $e_b(t)$ depends on the speed of the motor shaft, ω_m. It also opposes current flow and K_m. As demonstrated below,

$$e_b(t) = K_m \omega_m(t) \qquad (1)$$

The objectives of the experiments are to:

- Investigate two PID controller schemes (PV Position Control and PI Speed Control).
- Control the transient and steady-state dynamics of the servo motor using the controllers.

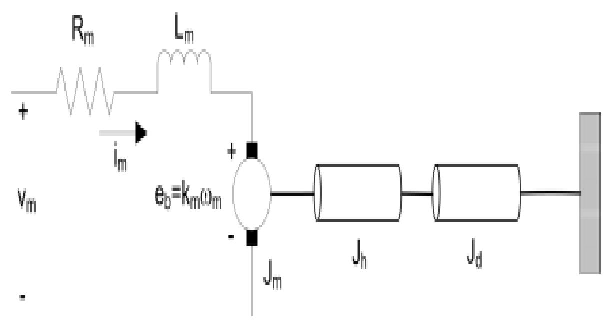

Fig. 2.QUBE-Servo Load and DC Motor.

2.2 PID control

2.3 Table 1: Electrical and Mechanical Parameters of Quanser QUBE-Servo Mechanism.

Symbol	Quantity	Description
DC Motor Parameters		
R_m	6.5Ω	Terminal Resistance
K_m	0.036 V/(rad/s)	Motor back emf Constant
K_t	0.036 N-m/A	Torque Constant
J_m	4.0 x 10^{-6} g-km^2	Rotor Inertia
L_m	0.85 mH	Rotor Inductance
m_h	0.0087 kg	Load Hub Mass
J_h	1.07 x 10^{-6} kg-m^2	Load Hub Inertia
r_h	0.0111 m	Radius of Disk Load
Load Parameters		
r_d	0.0248 m	Radius of Disk Load
m_d	0.054 kg	Mass of Disk Load

The mathematical expression for classic PID controller is given in (2) as follows,

$$G(t) = K_p e(t) + K_i \int_0^t e(t)\,dt + K_d \frac{d}{dt} e(t) \qquad (2)$$

The proportional term (P) is the statement of the present current error, the integral term is dependent on past error and the differential term gives the forecast of upcoming errors. It should be noted that the PID controller expressed above may not give satisfactory response when used for real world systems due to presence of measurement noise in measured signal.

2.4 PD position control

The proportional-derivative (PD) servo position control is a substitute of the proportional velocity (PV) controller, which is a variant of the classic PD controller. Instead of feeding back the velocity error, only the negative velocity is fed back in PV control. Furthermore, to supress measurement noise, a first order low pass filter is used adjacent to the derivative term forming a combination resulting in high pass filter. This high pass filter will be used instead of a direct derivative. The mathematical expression for PV control is given in (3),

$$U(t) = K_p\big(r(t) - y(t)\big) - K_d \dot{Y}(t) \qquad (3)$$

Where,$K_p$is the proportional gain,$K_d$represents the derivative (velocity) gain. Fig. 3 shows a typical block diagram of a PD position control. In Fig. 3,y = $\theta_m(t)$

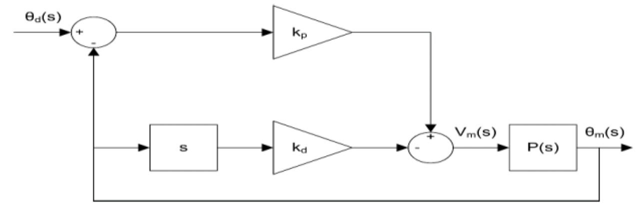

Fig. 3. Block Diagram of PV Controller.

represents load shaft angle,r = $\theta_d(t)$ means reference point, and finally u = $V_m(t)$ denotes motor input voltage. Assuming zero initial conditions i.e. $\theta_m(0^-) = 0$ and $\dot{\theta}_m(0^-) = 0$. Then, the closed loop transfer function of the servo is expressed in (4).

$$\frac{Y(s)}{R(s)} = \frac{KK_p}{\tau s^2 + (1 + KK_d)s + KK_p} \qquad (4)$$

2.5 PI speed control

This PI uses proportional term (K_p) to track and minimize error, integral term (K_i) to compensate forsteady state error. With this control structure, an acceptable performance can be achieved for simple systems. Conversely, some problems (like offset error, overshoot and long settling time) can manifest in non-linear systems. The linear characteristic of the PI controller is modelled as the mathematical expression in (5):

$$U(t) = K_p(r(t) - y(t)) + K_i \int_0^t (r(t) - y(t))\,dt \qquad (5)$$

Where, *r (t)* denotes the reference input, *u(t)* represents the control signal, and *y(t)* denotes the output quantified.

2. RESULTS

3.1 QUBE servo proportional-velocity (PV) control

In LabVIEW, the PV controller was modelled such the derivative term of the controller is in series with a low pass filter forming a high pass filter [150s/(s+150)]. The reference angle was set to 0.5 rad at 0.4 Hz. The virtual instrument was run by settings K_d = 0 and K_p = 2.5v/rad. Fig.4 indicates the performance response of

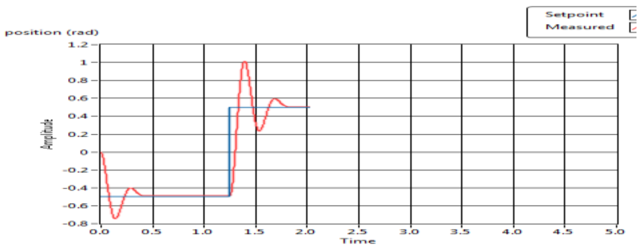

Fig. 4. Performance Response of QUBE-Servo Load and DC Motor.

the system. Thepeak time, percentage overshoot of the system wereobtained as follows: $Y_{max} = 1.015$, $SSV = 0.503, t_{max} = 1.394, INpoint = -0.485, and\ t_0 = 1.252$. Then using the relationship given in (6), the percentage overshoot and peak time were calculated as M_p = 51.9%, and t_p = 0.142 s respectively.

$$M_p(\%) = 100 \times \frac{(Y_{max} - SSV)}{SSV - INpoint} \qquad (6)$$

To investigate the effects of K_p on the control of the servo position, K_d was kept constant at 0 while varying K_p from 1 to 4. Table 2 shows a summary of the measurements taken from the responses recorded. Similarly, the effect of the K_d on the response was also studied. Table 3 shows a summary of the measurements recorded from each response.

Table 2: Summary of Measured Responses forVarying K_P while Setting $K_D = 0$.

K_D = 0.000				
t_p(s)	0.238	0.162	0.128	0.108
M_p (%)	24.660	40.786	60.729	60.622
K_P	1.000	2.000	3.000	4.000

Table 3: Summary of Measured Responses for Varying K_D and Setting $K_P = 2.5$.

K_P = 2.500					
t_p(s)	0.142	0.152	0.168	0.204	0.236
M_p (%)	37.750	14.530	1.700	0.000	0.000
K_D	0.030	0.060	0.090	0.120	0.150

3.2 QUBE servo proportional-integral (PI) speed control

A closed-loop PI speed control is implemented in LabVIEW as shown in Fig. 5. The controller quantifies the speed of the motor with these settings K_p = 0.2 and K_d = 0. In aneffort to improve the closed loop response, K_p and K_d of the system, were varied and the effects are summarized in Table 3. The controller was tuned until a response with minimal overshoot was obtained when K_p = 1.6 and K_d = 0.45. Similarly, controller was tuned to achieve a minimum settling time at K_p = 0.5 and K_d = 1.0. The systems response is shown in Fig. 6.

3. DISCUSSION

Results from Table 2 indicate that as the proportional gain (K_p) rises, there is increase in overshoot, in contrast to the peak time which declines.Also, it can be seen from Table 3 that as the derivative gain (K_d) upsurges at constant (K_p), (M_p) declined considerably until it reached zero (at K_d = 0.12 and K_d = 0.15). In contrast, the peak time increases linearly in proportion to the derivative gain. The overall trend result summarized in Table 4.On one hand, the results from Table 4 shows a direct variation between the proportional gain (K_p) and percentage overshoot; while on the other hand, the peak time shows an inverse variation. When the derivativegain increased, the opposite trend was noticed. An increase in the integral gain of the PI speed controller resulted in an increase in the steady-state error, overshoot, and settling time. Similarly, an increase in proportional gain has the same effect, except for the steady state error (it decreased instead). These trends are depicted in Table 5. The equations illustrate that an increase in the gain translate to decrease in steady state error and eventually approaching zero. Its challenges include overshoot, long settling time, and steady-state error when a significant increase in the integral term is registered.

In the experiment, the performance of PV position and PI speed controllers were investigated by studying the impact of the individual gains on the dynamics of a given systems. For the PV position controller, an

Table 4: Effect of Increasing K_p and K_I on the System Response.

Parameter	t_p	M_p
Increasing K_d	Increases	Decreases
Increasing K_p	Decreases	Increases

Table 5: Effect of IncreasingK_p and K_D on the Position Response.

Speed Response	Steady State Error	Settling Time	Overshoot
Growing (K_P)	Drops	Rises (Slightly)	
Growing (K_I)	Increases Significantly	Rises	Rises

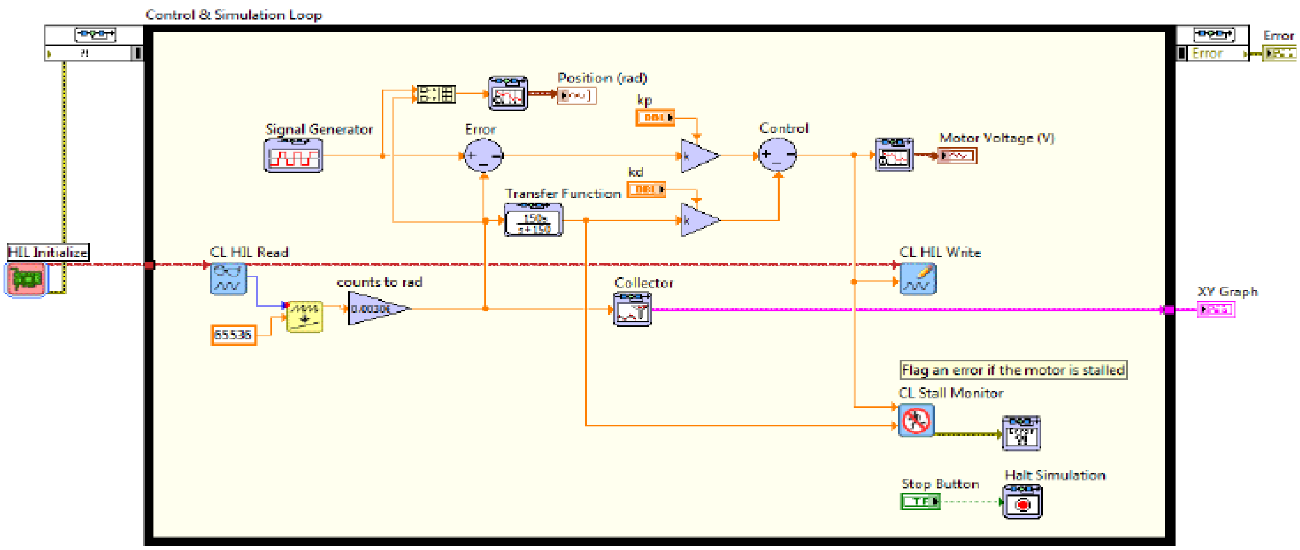

Fig. 5 System Closed-loop Speed (PI) Controller

increase in the derivative gain resulted in a decrease in the its peak time while percentage overshoot increases. The main drawback (measurement noises) of this controller was addressed by feeding back negative velocity instead of the velocity error and using high passfilter (incorporated in its design) to filter out the noise signals. An increase in the integral gain of the PI speed controller translates to an increase in steady-state error overshoot, settling time. A similar trend was observed with an increase in proportional gain, the only exception is the steady-state error which showed a decreasing trend (which can be due to lack of derivative term). Nevertheless, for systems with non-complex dynamics, optimal performance can still be obtained from the controller.

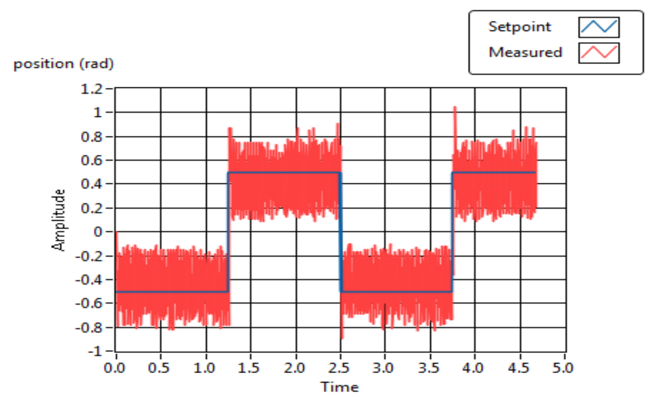

Fig. 6. Response of the Settling Time (Minimum).

4. CONCLUSION

This work performed an assessment of some PID-variants for control of UAV compliant servos using a Quanser QUBE testbench. The obtained resultsshowed that these controllers together with the servos have reasonable performance with optimal cost/benefit ratio making them useful on UAVs and a range of high precision applications.

REFERENCES

[1] M. F. Rahman, S. Fan, Y. Zhang, and L. Chen, "A Comparative Study on Application of Unmanned Aerial Vehicle Systems in Agriculture," *Agriculture* , vol. 11, no. 1. 2021, doi: 10.3390/agriculture11010022.

[2] P. Radoglou-Grammatikis, P. Sarigiannidis, T. Lagkas, and I. Moscholios, "A compilation of UAV applications for precision agriculture," *Comput. Networks*, vol. 172, p. 107148, 2020, doi: https://doi.org/10.1016/j.comnet.2020.107148.

[3] H. Shakhatreh *et al.*, "Unmanned Aerial Vehicles (UAVs): A Survey on Civil Applications and Key Research Challenges," *IEEE Access*, vol. 7, pp. 48572–48634, 2019, doi: 10.1109/ACCESS.2019.2909530.

[4] T. Alladi, V. Chamola, Naren, and N. Kumar, "PARTH: A two-stage lightweight mutual authentication protocol for UAV surveillance networks," *Comput. Commun.*, vol. 160, pp. 81–90, 2020, doi: https://doi.org/10.1016/j.comcom.2020.05.025.

[5] D. C. Tsouros, S. Bibi, and P. G. Sarigiannidis, "A Review on UAV-Based Applications for Precision Agriculture †," 2019, doi: 10.3390/info10110349.

[6] R. Czyba and G. Szafranski, "Control Structure Impact on the Flying Performance of the Multi-Rotor VTOL Platform - Design, Analysis and Experimental Validation," *Int. J. Adv. Robot. Syst.*, vol. 10, no. 1, p. 62, Jan. 2013, doi: 10.5772/53747.

[7] R. P. Borase and D. K. M. S. Y. S. S. N. Pawar, "A review of PID control , tuning methods and applications," *Int. J. Dyn. Control*, no. June, 2020, doi: 10.1007/s40435-020-00665-4.

[8] J. B. Song, Y. S. Byun, J. S. Jeong, J. Kim, and B. S. Kang, "Experimental study on cascaded attitude angle control of a multi-rotor unmanned aerial vehicle with the simple internal model control method," *J. Mech. Sci. Technol.*, vol. 30, no. 11, pp. 5167–5182, 2016, [Online]. Available: http://inis.iaea.org/search/search.aspx?orig_q=RN:48049476.

[9] R. DeMott, "Development of a Flexible FPGA-Based Platform for Flight Control System Research," 2010.

[10] H. Chao, Y. Cao, and Y. Chen, "Autopilots for Small Unmanned Aerial Vehicles: A Survey," *Int. J. Control Autom. Syst.*, vol. 8, pp. 36–44, Feb. 2010, doi: 10.1007/s12555-010-0105-z.

[11] A. A. Hoshu, L. Wang, A. Fisher, and A. Sattar, "Cascade control for heterogeneous multirotor UAS," *Int. J. Intell. Unmanned Syst.*, vol. ahead-of-p, no. ahead-of-print, Jan. 2021, doi: 10.1108/IJIUS-02-2021-0008.

[12] A. A. Hoshu, A. Fisher, and L. Wang, "Cascaded Attitude Control For Heterogeneous Multirotor UAS For Enhanced Disturbance Rejection," in *2019 Australian & New Zealand Control Conference (ANZCC)*, 2019, pp. 110–115, doi: 10.1109/ANZCC47194.2019.8945696.

[13] O. Mofid and S. Mobayen, "Adaptive sliding mode control for finite-time stability of quad-rotor UAVs with parametric uncertainties," *ISA Trans.*, vol. 72, pp. 1–14, 2018, doi: https://doi.org/10.1016/j.isatra.2017.11.010.

[14] H. Bouadi and M. Tadjine, "Nonlinear observer design and sliding mode control of four rotor helicopter," *Int J. Eng. Appl. Sci.*, vol. 3, Jan. 2007.

[15] H. Bouadi, M. Bouchoucha, and M. Tadjine, "Sliding Mode Control based on Backstepping Approach for an UAV Type-Quadrotor," *Int. J. Appl. Math. Comput. Sci.*, vol. 4, pp. 12–17, Jan. 2007.

[16] R. Garrido and R. Miranda, "DC servomechanism parameter identification: A closed loop input error approach," *ISA Trans.*, vol. 51, no. 1, pp. 42–49, 2012, doi:

https://doi.org/10.1016/j.isatra.2011.07.003.

[17] A. Arfaoui, "Unmanned Aerial Vehicle: Review of Onboard Sensors, Application Fields, Open Problems and Research Issues," *Aymen Arfaoui Int. J. Image Process.*, no. 11, p. 12, 2017.

[18] R. Bhimte, K. Bhole-Ingale, P. Shah, and R. Sekhar, "Precise Position Control of Quanser Servomotor using Fractional Order Fuzzy PID Controller," in *2020 IEEE Bombay Section Signature Conference (IBSSC)*, 2020, pp. 58–63, doi: 10.1109/IBSSC51096.2020.9332216.

[19] P. Shah and S. Agashe, "Review of fractional PID controller," *Mechatronics*, vol. 38, pp. 29–41, 2016, doi: https://doi.org/10.1016/j.mechatronics.2016.06.005.

[20] H. Delavari, R. Ghaderi, A. Ranjbar, and S. Momani, "Fuzzy fractional order sliding mode controller for nonlinear systems," *Commun. Nonlinear Sci. Numer. Simul.*, vol. 15, no. 4, pp. 963–978, 2010, doi: https://doi.org/10.1016/j.cnsns.2009.05.025.

[21] S. Das, I. Pan, S. Das, and A. Gupta, "A novel fractional order fuzzy PID controller and its optimal time domain tuning based on integral performance indices," *Eng. Appl. Artif. Intell.*, vol. 25, no. 2, pp. 430–442, 2012, doi: https://doi.org/10.1016/j.engappai.2011.10.004.

[22] L. Liu, F. Pan, and D. Xue, "Variable-order fuzzy fractional PID controller," *ISA Trans.*, vol. 55, pp. 227–233, 2015, doi: https://doi.org/10.1016/j.isatra.2014.09.012.

[23] V. Kumar and K. P. S. Rana, "Nonlinear adaptive fractional order fuzzy PID control of a 2-link planar rigid manipulator with payload," *J. Franklin Inst.*, vol. 354, no. 2, pp. 993–1022, 2017, doi: https://doi.org/10.1016/j.jfranklin.2016.11.006.

[24] .-Y. Cao, J. Liang, and B.-G. Cao, "Optimization of fractional order PID controllers based on genetic algorithms," in *2005 International Conference on Machine Learning and Cybernetics*, 2005, vol. 9, pp. 5686-5689 Vol. 9, doi: 10.1109/ICMLC.2005.1527950.

[25] J. Cao and B. Cao, "Design of Fractional Order Controllers Based on Particle Swarm Optimization," in *2006 1ST IEEE Conference on Industrial Electronics and Applications*, 2006, pp. 1–6, doi: 10.1109/ICIEA.2006.257091.

[26] P. Shah and S. Agashe, "Experimental analysis of fractional PID controller parameters on time domain specifications," *Prog. Fract. Differ. Appl.*, vol. 3, no. 2, pp. 141–154, 2017, doi: 10.18576/pfda/030205.